STACKING DEFECTS IN SYNTHETIC AND METEORITIC HIBONITES: IMPLICATIONS FOR HIGH-TEMPERATURE PROCESSES IN THE SOLAR NEBULA. J. Han[1,2], L. P. Keller[2], A. J. Brearley[3], and L. R. Danielson[4]. [1]Lunar and Planetary Institute, Houston, TX 77058, USA (jangmi.han@nasa.gov), [2]ARES, NASA/JSC, Houston, TX 77058, USA, [3]Department of Earth and Planetary Sciences, University of New Mexico, Albuquerque, NM 87131, USA, [4]Jacobs JETS, NASA/JSC, Houston, TX 77058, USA.

Introduction: Hibonite ($CaAl_{12}O_{19}$) is a primary, highly refractory phase occurring in many Ca-Al-rich inclusions (CAIs) from different chondrite groups, except CI chondrites [1]. Hibonite is predicted to be one of the earliest minerals to condense during cooling of the solar nebula at higher temperatures than any other major CAI mineral [2]. Therefore, hibonite has great potential to reveal the processes and conditions of the very early, high-temperature stages of the solar nebular evolution.

Previous microstructural studies of hibonite in CAIs and their Wark-Lovering (WL) rims showed the presence of numerous stacking defects in hibonite. These defects are interpreted as the modification of the stacking sequences of spinel and Ca-containing blocks within the ideal hexagonal hibonite structure [3,4], as shown by experimental studies of reaction-sintered ceramic $CaO-Al_2O_3$ compounds [5]. We performed preliminary experiments in the $CaO-Al_2O_3-MgO$ system to understand the formation processes and conditions of defect-structured hibonite found in meteorites.

Methods: Two experiments were prepared by allowing pure alumina crucibles to react with (1) $2CaO-Al_2O_3$ eutectic melt and (2) $2CaO-Al_2O_3$ eutectic melt with 5 wt% MgO in a high-temperature box furnace at 1,530°C for 4 hours, followed by air quenching. The run products were cut, mounted in epoxy, and polished for detailed petrologic and mineralogical descriptions using a JEOL 7600F field emission SEM and a JEOL 8530F electron microprobe. A TEM section was extracted from hibonite in the reaction zone of the run products using a FEI Quanta 3D Field Emission Gun SEM/FIB instruments. The sections were then examined for micro-to-nanometer scale structural and chemical characterization by a JEOL 2500SE field-emission scanning TEM equipped with a Thermo-Noran thin window energy dispersive X-ray (EDX) spectrometer.

Results: *Experiment (1) in the CaO-Al₂O₃ system.* The reaction zone adjacent to the alumina consists of distinct mineral layers of a series of calcium aluminates from hibonite (5-60 µm thick), grossite (30-70 µm thick), to krotite with a melt residue (Fig. 1a). Hibonite, grossite, and krotite are pure $CaAl_{12}O_{19}$, $CaAl_4O_7$, and $CaAl_2O_4$, respectively.

The FIB section 1-1 consists of compact aggregates of hibonite laths that share common elongation directions with rounded corundum inclusions. Electron diffraction patterns of hibonite grains are well-defined

with uniform *d*-spacings, indicative of the presence of ordered, stoichiometric hibonite. Most hibonite crystals are free of defects, but a few grains contain a very low density of stacking defects parallel to the *c* axis. Lattice fringe images of hibonite grains show isolated, single layers of 2.6 nm (001) spacing within ordered hibonite of 2.2 nm (001) spacing. Quantitative EDX analyses show that hibonite grains have a uniform composition of pure $CaAl_{12}O_{19}$, but defect-rich areas in hibonite show Ca deficiencies up to ~8 mol%.
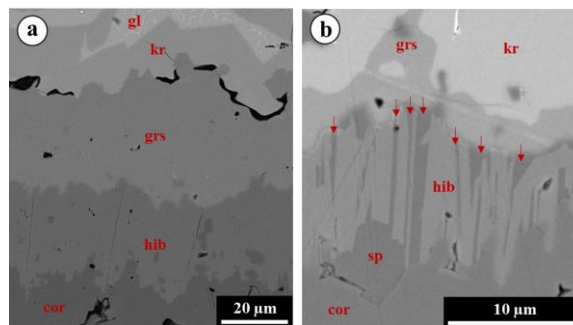

Figure 1. Backscattered electron (BSE) images of the run products of experiment (1) (a) and experiment (2) (b), showing a similar sequence of corundum (cor), hibonite (hib), grossite (grs), and krotite (kr)+glass (gl). In (b), spinel (sp) indicated by arrows is intergrown with hibonite.

Experiment (2) in the CaO-Al₂O₃-MgO system. Like experiment (1), this experiment produced the similar mineral sequence of hibonite (5-25 µm thick), grossite (1-15 µm thick), to krotite with a melt residue (Fig. 1b). An important difference is that the addition of Mg stabilized spinel in two occurrences; (1) spinel laths intergrown with hibonite and (2) euhedral spinel crystals in the melt residue. Hibonite contains 0.16-0.25 wt% MgO. Grossite and krotite are pure $CaAl_4O_7$ and $CaAl_2O_4$, respectively. While spinel grains in the krotite-melt mixture are nearly pure $MgAl_2O_4$, spinel grains intergrown with hibonite show significant enrichments in Al_2O_3 with 2.14-2.20 Al cations per 4 oxygen anions.

The FIB section 2-1 consists of compact intergrowths of randomly-oriented hibonite laths and spinel grains (Fig. 2). In contrast to defect-free spinel, hibonite contains abundant stacking defects parallel to the *c* axis. Electron diffraction patterns of hibonite show strong streaking along the *c* axis, indicating the presence of stacking disorder. The stacking disorder is readily apparent in lattice fringe images of hibonite

grains that show random intergrowths of various (001) spacing ranging from 2.6 nm to 3.7 nm within prominent 2.2 nm (001) spacing. In addition, a crystallographic orientation relationship exists between hibonite and spinel. Analysis of electron diffraction patterns from two sets of hibonite and spinel yields $(001)_{hibonite}//(111)_{spinel}$. Quantitative EDX analyses reveal that defect-rich areas in hibonite are enriched in MgO relative to defect-free, ordered areas in hibonite. Spinel is a solid solution of $Al_{8/3}O_4$-$MgAl_2O_4$ with ~20 mol% excess Al_2O_3.
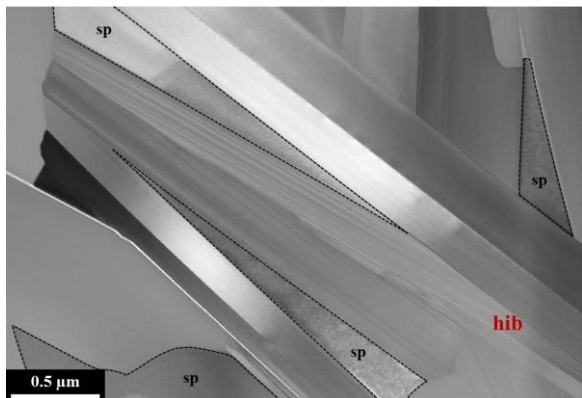

Figure 2. Bright-field scanning TEM image of hibonite laths intergrown with spinel (outlined in dotted lines) in FIB 2-1.

Discussion: The hibonite in the run products has several similarities to that in CAIs and their WL rims; (1) the presence of stacking defects and correlated compositional variations in hibonite [3,4,6,7], (2) the crystallographic orientation relationships between intergrown hibonite and spinel [4,6], and (3) the presence of excess Al_2O_3 in spinel [8,9].

The presence of stacking defects found in hibonite from the two experiments can be explained by the arrangement and distribution of two distinct polyhedral layers, spinel (S) and Ca-containing (C) layers, normal to the c axis in hibonite. The ideal hibonite structure consists of a stacking sequence of SCS*C*, where S* and C* are rotated 180° around the c axis relative to S and C, respectively [10]. A unit cell of the perfectly ordered sequence of SCS*C* in hibonite has a 2.2 nm (001) spacing. This spacing is predominantly observed in areas without any defects in synthetic and meteoritic hibonite [3,4,6,7]. However, the basic structural S and C blocks can be stacked in different ratios, yielding a change in unit formula, composition, and length of the c axis [5]. In FIB 1-1, hibonite contains few layers of 2.6 nm (001) spacing, and a decrease in the CaO contents was linked to these layers, indicative of the rare occurrence of thicker S blocks consisting of six rather than four oxygen planes (i.e., SSC) in stoichiometric hibonite. In addition, MgO-bearing hibonite in FIB 2-1

contains a higher density of stacking defects consisting of a range of spacings from 2.6 nm to 3.7 nm, and defect-rich areas show relatively increased MgO contents. Similarly, hibonite in ALHA77307 hibonite-spinel CAIs with ≤3 wt% MgO contains a range of (001) spacings from 4.8 nm to 11.4 nm linked to an increase in the MgO contents [4]. Collectively, these observations indicate that the introduction of Mg during the formation of hibonite stabilized the formation of wider S blocks due to the substitution of Mg with Al on two tetrahedral sites in the S blocks [11].

The occurrence of spinel in crystallographic continuity with MgO-bearing hibonite in FIB 2-1 demonstrates that spinel nucleated onto hibonite due to their structural similarity [12]. A significant excess of Al_2O_3 in spinel intergrown with hibonite is observed in FIB 2-1 and is consistent with a thermodynamic mixing model that predicts up to 30 mol% $Al_{8/3}O_4$ in $Al_{8/3}O_4$-$MgAl_2O_4$ spinels at 1530°C [13]. The presence of corundum as a reactant and the high Al_2O_3 contents of coexisting melt in experiment (2) appear to increase the solubility of Al_2O_3 in $MgAl_2O_4$ spinel [9,13], forming the solid solution series of $Al_{8/3}O_4$-$MgAl_2O_4$ spinel. Additionally, in comparison with experiment (1) that produced fairly similar widths of hibonite and grossite, experiment (2) produced a significantly narrower layer of grossite relative to that of intergrown hibonite and spinel. The depletion in Al due to the formation of Al-rich spinel may have limited the formation of grossite.

Conclusions: Our preliminary experiments in the CaO-Al_2O_3 and CaO-Al_2O_3-MgO systems produced hibonite that contains stacking defects similar to those observed in meteoritic hibonites. A much higher defect density in MgO-bearing hibonite suggests that the substitution of Mg with Al in the S blocks stabilized the formation of wider S blocks (i.e., defects). The observed structural and compositional similarities between synthetic and meteoritic hibonite suggest that the metastable, defect-rich hibonite is more stable than stoichiometric hibonite in high-temperature melts.

References: [1] MacPherson G.J. (2014) Treatise on Geochemistry II vol.1 pp.139-179. [2] Ebel D.S. (2006) MESS2 pp.253-277. [3] Keller L.P. (1991) AGU 72, 141. [4] Han J. et al. (2015) MAPS 50, 2121-2136. [5] Schmid H. & De Jonghe L.C. (1983) Philos. Mag. A 48, 287-297. [6] Han J. et al. (2015) 46th LPSC abtract #2702. [7] Han J. et al. (2015) MAPS 50, A153. [8] El Goresy A. et al. (1984) GCA 48, 2283-2298. [9] Simon S.B. et al. (1994) GCA 58, 1937-1949. [10] Nagashima M. et al. (2010) Mineral. Mag. 74(5), 871-885. [11] Doyle P.M. et al. (2014) AM 99, 1369-1382. [12] Beckett J.R. & Stolper E. (1994) Meteoritics 29, 41-65. [13] Sack R.O. (2014) Am. J. Sci. 314, 858-877.